



Repair of Skin Defects with Electrospun Collagen/Chitosan and Fibroin/Chitosan Compound Nanofiber Scaffolds Compared with Gauze Dressing

PiJun Yu¹, JiAn Guo¹, JunJie Li¹, Xiao Shi¹, LuPing Wang¹, Wei Chen^{1,*}, and XiuMei Mo^{2,*}

¹Shanghai Eighth People's Hospital, Shanghai, 200235, China

²College of Chemistry, Chemical Engineering and Biotechnology, Donghua University, Shanghai, 201620, China

Skin wound repair by biomaterials has been extensively investigated. However, there have been relatively few reports on the use of electrospun nanofibers as novel biodegradable materials in skin defect repair. In this context, we evaluated electrospun scaffolds of collagen/chitosan (CL/CS) nanofibers at an 80:20 ratio and silk fibroin/chitosan (SF/CS) nanofibers at a 50:50 ratio. To test the biocompatibility of these two novel nanofiber scaffolds, we cocultured the materials with cells *in vitro* and applied the scaffolds in an animal skin defect repair model *in vivo*. The morphology of the electrospun nanofiber scaffolds was observed by field emission scanning electron microscopy. The proliferation of Sprague-Dawley (SD) rat skin fibroblasts (FBs) and keratinocytes (KCs) seeded on tissue culture plastic and CL/CS and SF/CS scaffolds was studied using methylthiazol tetrazolium assays. The morphology of cells on the nanofiber scaffolds was investigated by scanning electron microscopy. *In vivo*, the biocompatibility of the compound nanomaterials with the surface of the wounded rat skin was assessed by conducting macroscopic observations and hematoxylin and eosin staining of wound tissue samples. The results showed that the FBs and KCs isolated from SD rat skin proliferated well on and within the nanofiber scaffolds. Compared with the control group (gauze dressing), the CL/CS and SF/CS scaffolds had good biocompatibility and promoted wound healing. Therefore, CL/CS and SF/CS nanofiber scaffolds may be good candidates for skin tissue engineering applications.

Keywords: Fibroblasts, Keratinocytes, Collagen/Chitosan Nanofiber Scaffold, Silk Fibroin/Chitosan Nanofiber Scaffold, Wound Healing.

1. INTRODUCTION

Wound healing is a restorative process that is necessary for tissue repair and typically comprises a continuous sequence of inflammatory and repair activities in which epithelial, endothelial, and inflammatory cells, platelets and fibroblasts briefly interact in order to resume their normal functions. This healing process consists of four different and overlapping phases, namely, inflammation, granulation tissue formation, matrix remodeling and reepithelialization.¹

To restore the function of the skin after damage and to facilitate the wound healing process, autologous scaffolds are commonly used to repair the skin while avoiding immune rejection.² However, extensive skin damage beyond the capabilities of conventional graft extraction methods requires the rapid *in vitro* manufacture of biocompatible materials to promote wound healing.^{3–5}

After being transplanted onto the site of injury, these biocompatible materials play the role of the extracellular matrix (ECM) to prevent fluid loss and infection.

Collagen (CL), one of the main types of protein in mammals, is a basic component of the three-dimensional network structure of native ECM and is composed of nano-scaled fibrils. CL has been utilized in biomaterials for a wide variety of applications, including drug delivery carriers,⁶ wound dressings⁷ and tissue engineering scaffolds,⁸ due to its advantages of non-immunogenicity, excellent biocompatibility and biodegradability. Silk fibroin (SF) is a natural protein that has good biocompatibility, oxygen and water vapor permeability, and biodegradability; in addition, it elicits a lower inflammatory response than CL and is commercially available at a relatively low cost.^{9–11} As such, SF has been widely used in tissue engineering. Chitosan (CS) is an abundant polysaccharide derived from chitin. Because of its excellent biocompatibility, appropriate biodegradability,

*Authors to whom correspondence should be addressed.

excellent physicochemical properties and relatively low-cost commercial availability, chitosan has also been widely used in the pharmaceutical and medical fields.^{12,13} Studies have reported that CS and CL can form a composite system^{14,15} with complementary and synergistic performance.

Electrospinning is a versatile technique that has been increasingly used as an efficient processing method for manufacturing fibers with a diameter ranging from nano- to micrometers.^{16–18} Consequently, it is very easy to generate nanofibers mimicking the structure of the ECM via electrospinning. Previous studies have described electrospun CL-CS complexes and their intermolecular interactions,^{19–22} as well as electrospun SF/CS complexes.²³ However, for application as tissue engineering scaffolds, the biocompatibility and feasibility of electrospun CL/CS and SF/CS nanofibers should be further studied both *in vitro* and *in vivo*.

This study aimed to prepare CL/CS and SF/CS nanofiber scaffolds via electrospinning, assess the biocompatibility of the scaffolds both *in vitro* and *in vivo*, and evaluate the effects of the scaffolds on wound healing in a skin defect model.

2. EXPERIMENTAL METHODS

2.1. Materials

Type I CL (mol. wt., $0.8\text{--}1 \times 10^5$ Da) was purchased from Sichuan Mingrang Bio-Tech Co., Ltd. (China), *Bombyx mori* silkworm cocoons were purchased from Jiaxing Silk (China), and CS (85%, deacetylated, $M_n \approx 10^6$) was purchased from Jinan Haidebei Marine Bioengineering Co., Ltd. (China). Regarding the solvents, 1,1,1,3,3,3-hexafluoroisopropanol (HFIP) used for dissolving CL was purchased from Fluorochem Ltd. (UK), and trifluoroacetic acid (TFA) used to dissolve the CS was obtained from Sinopharm Chemical Reagent Co., Ltd. (China). Glutaraldehyde (GTA), a crosslinking agent, was purchased at a concentration of 25% from Sinopharm Chemical Reagent Co., Ltd. (China). All culture media and reagents were purchased from Solarbio Biomedical Technology Inc. (China).

2.2. Electrospinning of CL/CS and SF/CS Scaffolds

CL and CS solutions were prepared at a concentration of 8% (w/v) by dissolving CL and CS in HFIP and HFIP/TFA (v/v, 90/10), respectively. Then, the CL/HFIP and CS/HFIP/TFA solutions were mixed at a ratio of 8:2 (CL/CS = 80/20, w/w). In the electrospinning process, the polymer solution was placed into a 5-ml syringe with a 21-gauge needle. A clamp connected a high-voltage power supply (JDF-1, China) to the needle, and a round piece of aluminum foil was used as the collector. The needle and collector were 13 cm apart, and nanofibers were deposited on the collector using an applied voltage of 16 kV and a solution feed rate of 0.8 ml/h. Cover slips 14 mm in diameter were also placed on aluminum foil targets to

collect nanofibers for the biocompatibility investigation. The nanofibers were dried and preserved in a vacuum oven at room temperature for 7 days.

The preparation of the SF/CS nanofiber scaffolds was very similar to that of the CL/CS nanofiber scaffolds.^{22,23} Before we prepared the SF/CS solution, we first prepared regenerated silk, as follows: raw silk was degummed with a 0.5% (w/w) Na_2CO_3 solution at 100 °C for 30 min and washed with distilled water. This process was repeated three times, and the silk was dried at 40 °C overnight. Next, the degummed silk was dissolved in a ternary solvent system of $\text{CaCl}_2/\text{H}_2\text{O}/\text{EtOH}$ solution (1/8/2 molar ratio) for 1 h at 70 °C. After dialysis with a cellulose tubular membrane (250-7u; Sigma) in distilled water for 3 days at room temperature, the SF solution was filtered and lyophilized to obtain regenerated SF sponges. Next, the SF was dissolved in HFIP at a concentration of 12% (w/v), and CS was dissolved in an HFIP/TFA mixture (v/v 90:10) at a concentration of 6% (w/v). Subsequently, the two solutions were blended at a 50:50 ratio with sufficient stirring at room temperature before electrospinning. A 2.5-ml plastic syringe with a 21-gauge, blunt-ended needle was filled with the solution and connected to a syringe pump (789100C; Cole-Pamer, USA) at a distance of 150 mm from the grounded collector. The solution was dispensed at a rate of 0.5–1.0 ml/h. An applied voltage of 20 kV was provided by a high-voltage power supply (BGG6358, BMEI Co., China).

Before being used in any of the experiments, the prepared CL/CS nanofiber mats were subjected to a crosslinking process by first placing them in a sealed desiccator. Next, 10 ml of a 25% GTA aqueous solution was placed in a Petri dish at the bottom of the desiccator while the nanofiber scaffolds remained on a perforated ceramic shelf in the middle of the desiccator. The samples were crosslinked in an atmosphere of water and GTA vapor at room temperature for 2 days and were then kept in a vacuum oven at room temperature.

2.3. Scaffold Morphology Characterization

Scaffold morphology was observed by field emission scanning electron microscopy (FE-SEM, S-4800, Japan). SEM images were analyzed using ImageJ software (National Institutes of Health). The average fiber diameter was determined by measuring 50 randomly chosen fibers.

2.4. Cell Culture

The isolation of primary SD rat dermal FBs was performed as follows. Fresh 4-week-old SD rat skin biopsies were washed using phosphate-buffered saline (PBS) with 1% (v/v) penicillin and streptomycin and were immersed in 75% ethanol for 10 minutes. The biopsies were then chopped into small pieces, which were immersed in 0.25% trypsin (Sigma, USA) in PBS 4 °C overnight. Subsequently, the samples were digested with 1.5 mg/ml type II collagenase (GIBCO, USA) in Dulbecco's modified

Eagle's medium (DMEM) at 37 °C for 3 hours. The harvested dermal FBs were maintained in DMEM supplemented with 10% (v/v) fetal bovine serum, 100 U/ml penicillin, and 100 mg/ml streptomycin in a humidified incubator at 5% CO₂ and 37 °C.

The isolation of primary SD rat KCs was performed as follows. Fresh 4-week-old SD rat skin biopsies were washed using PBS with 1% (v/v) penicillin and streptomycin and were immersed in 75% ethanol for 10 minutes. The biopsies were then chopped into small pieces and immersed in 0.25% trypsin/PBS at 4 °C overnight. Thereafter, the dermis was separated from the epidermis, and the epidermal tissue was digested in 0.25% trypsin/PBS for 10 minutes. The harvested KCs were maintained in defined keratinocyte serum-free medium (GIBCO, USA) containing 100 U/ml penicillin and 100 mg/ml streptomycin in a humidified incubator at 5% CO₂ and 37 °C.

The culture medium was changed every other day. Both cell lines were subcultured when the cells had become confluent.

2.5. Cell Proliferation

The biocompatibility and proliferative capacity of the CL/CS and SF/CS nanofibers was evaluated *in vitro*. Suspensions of fourth-passage FBs and KCs (1×10^5 cells/ml) were seeded and cultured on 96-well culture plates with and without CL/CS or SF/CS nanofibers at the bottom the wells. FBs and KCs cultured on tissue culture plastic alone or for one day with CL/CS and SF/CS nanofibers were used as the controls. After being cultured for 1, 3, 5, and 7 days, absorbance values determined by the methylthiazol tetrazolium (MTT) assay were measured and analyzed.

2.6. Cell Morphology

Fourth-passage FBs and KCs were seeded on CL/CS and SF/CS nanofibers using the same method described above. After one week of culture, the cells on the nanofibers were fixed by gradient ethanol dehydration and freeze-dried to be observed by SEM.

2.7. Wound Healing

First, SD rats were anesthetized, and a wound 2×1.5 cm² in size was made on the back of each rat. The wound was then dressed with a nanofiber scaffold, and gauze was placed on top of the scaffold. For the control group, the wound was only dressed with gauze. Each group included 15 rats. The general surveys of the wounds and H&E staining were performed on the 3rd, 7th, and 14th postoperative days. The experiments were performed with the approval of the Institutional Animal Ethics Committee.

2.8. Statistical Analysis

Statistical analyses were performed using Origin 7.5 (Origin Lab). The values (in at least triplicate) were averaged and expressed as the mean \pm standard deviation. Statistical

differences were determined by one-way ANOVA, and differences were considered statistically significant at $P < 0.05$.

3. RESULTS AND DISCUSSION

3.1. Morphology of the Materials

SEM images of the electrospun nanofibers comprising CL and CS at a ratio of 80:20 are shown in Figure 1(a). SEM images of the electrospun nanofibers comprising SF and CS at a ratio of 50:50 are shown in Figure 1(b). The fiber diameter measurements are shown in Figure 1(c); the CL/CS scaffolds had a fiber diameter of 417 ± 146 nm, and the SF/CS scaffolds had a fiber diameter of 516 ± 125 nm. The fiber diameters of the two scaffold types were not significantly different, and the morphologies of the two electrospun nanofiber scaffolds were similar.

3.2. Cell Proliferation

The cell proliferation capacity and biocompatibility of the CL/CS and SF/CS nanofiber scaffolds at different times were evaluated by MTT assays (Figs. 2(a, b)). Cells cultured on tissue culture plastic alone or for one day on CL/CS and SF/CS nanofiber scaffolds were used as controls. As shown in Figure 2(a), the FBs proliferated more rapidly in wells containing a CL/CS or SF/CS nanofiber scaffold. Figure 2(b) shows that the KCs also proliferated more rapidly in wells containing a CL/CS or SF/CS nanofiber scaffold. These results demonstrated the biocompatibility of the nanofiber scaffolds. Furthermore, the nanofiber structure may provide a three-dimensional space for cell growth, which suggests the potential for its future application in the construction of skin tissue. The growth rate of cells cultured on the nanofiber scaffolds was significantly different from that of cells cultured on tissue culture plastic alone on the 3rd, 5th, and 7th days, indicating that the nanofiber scaffolds have good biocompatibility.

3.3. Cell Morphology

The morphologies of the FBs and KCs as determined using an inverted microscope are shown in Figures 3(a and b), respectively. The FBs had a fusiform morphology, and the cell contours were clear. The KCs exhibited a cobblestone shape and colony-type growth, and the cell contours were clear. Figures 3(c and e) show SEM images of the morphology of FBs on the CL/CS and SF/CS nanofiber scaffolds, respectively, after 7 days of culture. The cells exhibited more integration with the nanofibers with increasing cell number. Figures 3(d and f) show SEM images of the morphology of KCs on CL/CS and SF/CS nanofiber scaffolds, respectively, after 7 days of culture. The cell contours were clear, and the shape of these cells was similar to that of cells grown on tissue culture plastic.

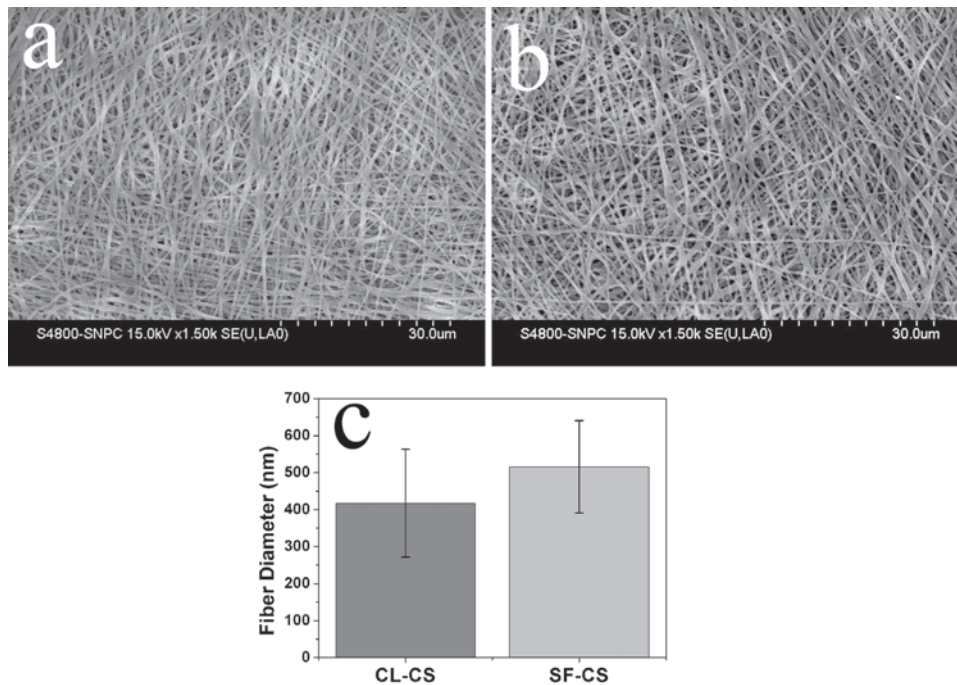


Fig. 1. SEM images of (a) CL/CS and (b) SF/CS scaffolds; (c) the fiber diameters of the CL/CS and SF/CS scaffolds.

3.4. Wound Healing

The general appearance of the wound surfaces after 3, 7, and 14 days of treatment with CL/CS and SF/CS nanofiber scaffolds is presented in Figures 4(a1 and a2), Figures 4(b1 and b2) and Figures 4(c1 and c2), respectively. The general appearance of wounds in the control group at the same time points is shown in Figures 4(a3, b3 and c3). The H&E staining results from the 3rd, 7th, and 14th days are shown in Figures 5(a, b and c), respectively.

The general condition of the wounds treated with the CL/CS and SF/CS nanofibers on the third postoperative day is displayed in Figure 4(a). In the CL/CS group, the wound surfaces were clean with no signs of infection. The margins of the wounds had slightly decreased (Fig. 4(a1)). In the SF/CS group, the wound surfaces were also clean and showed no signs of infection (Fig. 4(a2)). In the control group, the wound surfaces were red compared

with those in the two nanofiber groups (Fig. 4(a3)). The H&E staining results of the wounds in the CL/CS, SF/CS and control groups on day 3 are shown in Figure 5(a). Many capillaries were open and dilated, and there was a high degree of neutrophil infiltration. Necrotic tissue was observed in the wounds treated with CL/CS and SF/CS nanofibers (Figs. 5(a1, a2)). No significant differences were observed between the two nanofiber groups (Fig. 5(a3)).

The general condition on day 7 of the wounds treated with the nanofibers or the control is shown in Figure 4(b). The wound surfaces in the CL/CS group were clean with no signs of infection. Scabs were observed on the wound surfaces, and the margins of the wounds had greatly decreased (Fig. 4(b1)). The wound surfaces in the SF/CS group were less clean than those in the CL/CS group but had no signs of infection (Fig. 4(b2)). Of the three groups,

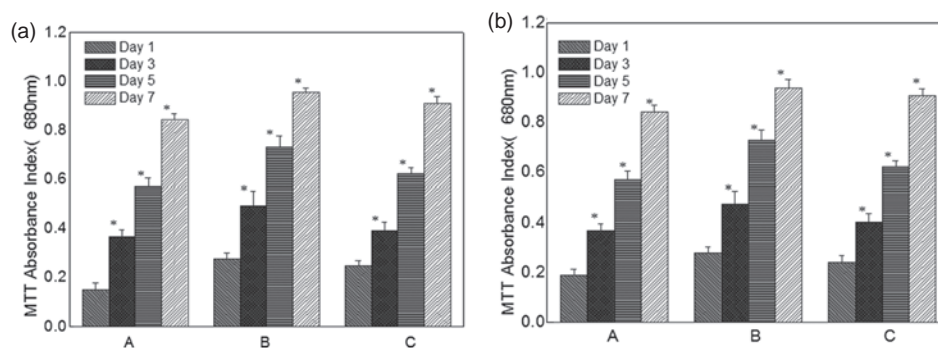


Fig. 2. Cell proliferation on the nanofiber scaffolds. (MTT Absorbance at 680 nm). (a) A: FBs; B: CL/CS + FBs; C: SF/CS + FBs (* $P < 0.05$). (b) A: KCs; B: CL/CS + KCs; C: SF/CS + KCs (* $P < 0.05$). (* $P < 0.05$; significant difference in cell growth after 3, 5, and 7 days of culture).

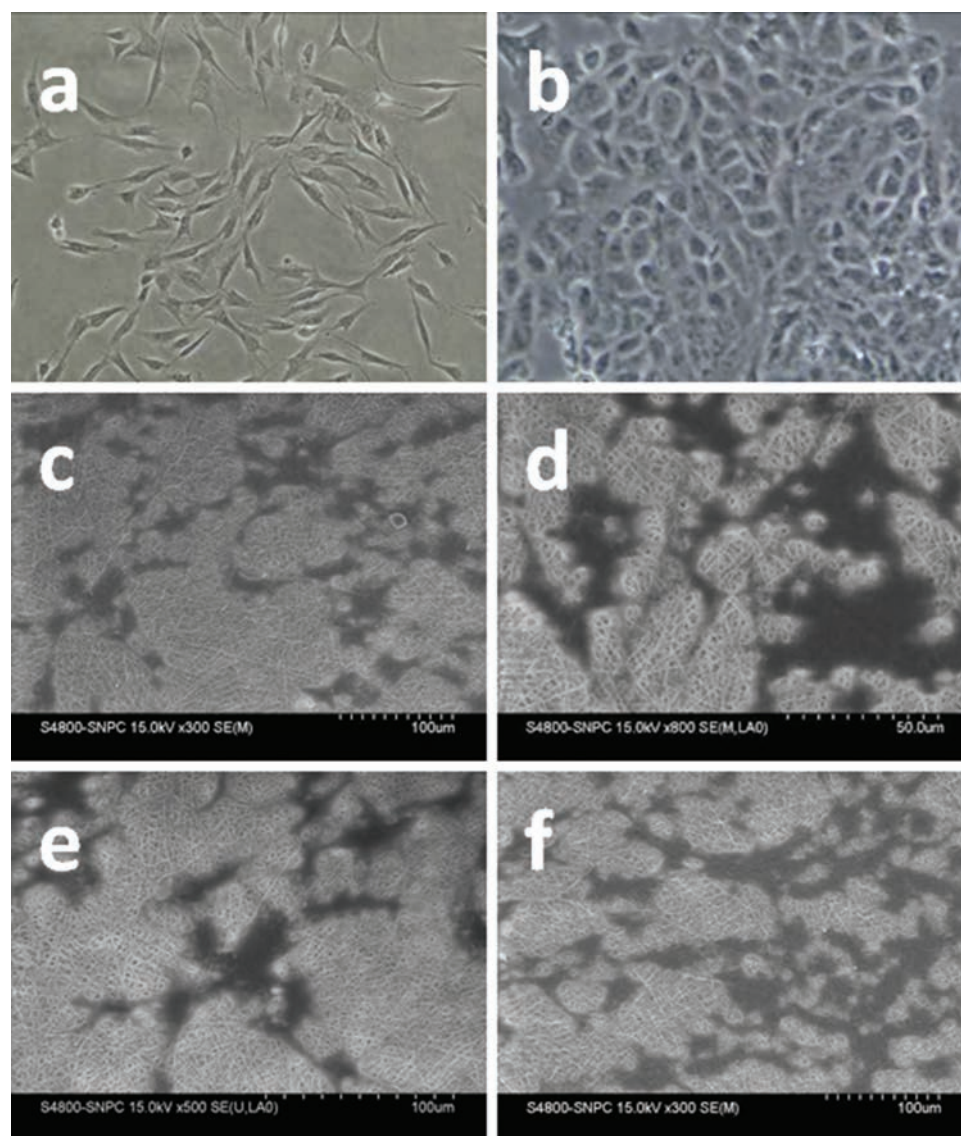


Fig. 3. (a) FBs; (b) KCs; (c) FBs on CL/CS nanofibers; (d) KCs on CL/CS nanofibers; (e) FBs on SF/CS nanofibers; (f) KCs on SF/CS nanofibers.

the wound surface area was largest in the control group (Fig. 4(b3)).

The H&E staining results of the wounds in the CL/CS, SF/CS and control groups on day 7 are shown in Figure 5(b). The number of opened and dilated capillaries was reduced, and the degree of neutrophil infiltration had also decreased. In addition, epithelial cells were observed on the CL/CS and SF/CS nanofiber membranes (Figs. 5(b1, b2)). The H&E staining results of the control group showed that many capillaries were still opened and dilated, and a considerable degree of neutrophil infiltration remained (Fig. 5(b3)).

The general condition of the wounds in the CL/CS, SF/CS and control groups at postoperative day 14 is shown in Figure 4(c). The wound surfaces in the CL/CS group were clean with no signs of infection. Scabs were observed on the wound surfaces, and the margins of

the wounds had greatly decreased such that the wound edges were touching (Fig. 4(c1)). The wound surfaces in the SF/CS group were clean with no signs of infection (Fig. 4(c2)). The control group showed poorer wound healing than the CL/CS and SF/CS groups (Fig. 4(c3)). The H&E staining results of the CL/CS, SF/CS and control groups at the fourteenth postoperative day are displayed in Figure 5(c). The numbers of open and dilated capillaries were reduced compared with those on the 3rd and 7th days, the degree of neutrophil infiltration had decreased, and epithelium had formed (Figs. 5(c1, c2)). The wound repair in the CL/CS and SF/CS groups was better than that in the control group (Fig. 5(c3)). Compared with the control, the CL/CS and SF/CS nanofiber scaffolds demonstrated good biocompatibility and promoted wound healing.

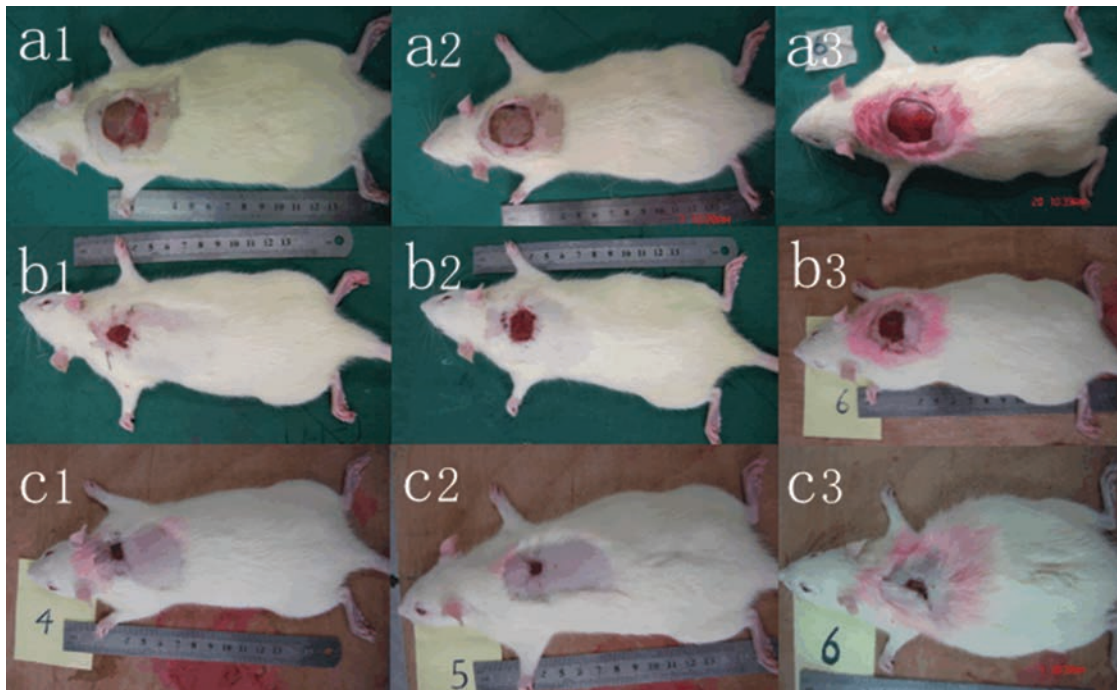


Fig. 4. General condition of the wounds in the CL/CS (1), SF/CS (2) and control (3) groups on the third (a), seventh (b), and fourteenth (c) postoperative days.

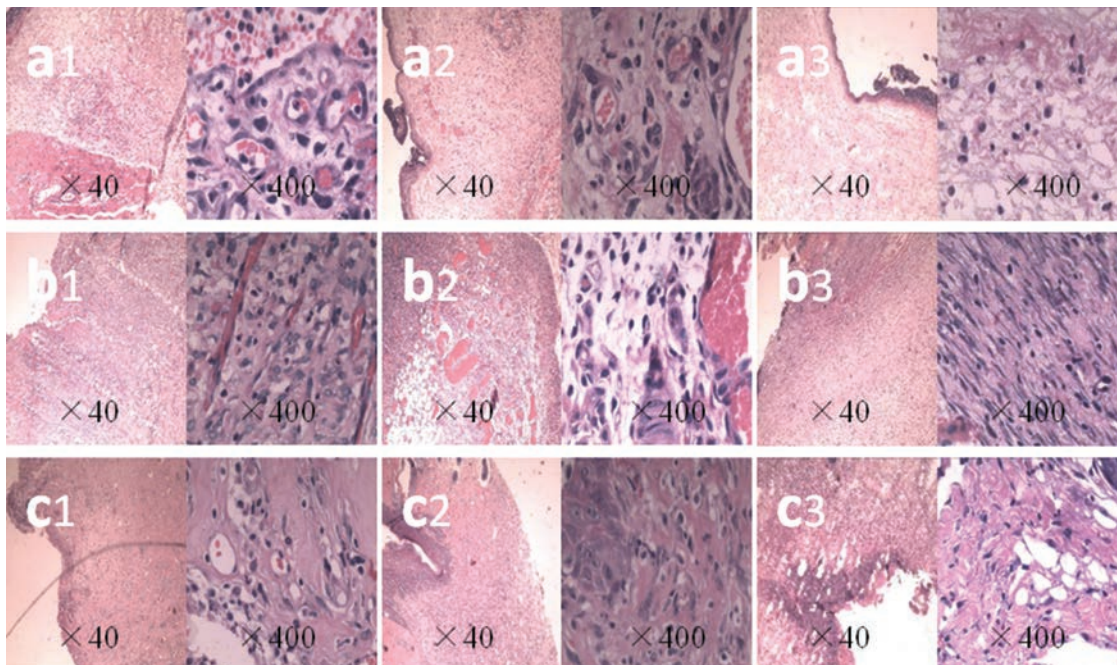


Fig. 5. H&E staining of wounds in the CL/CS (1), SF/CS (2) and control (3) groups on the third (a), seventh (b), and fourteenth (c) postoperative days.

4. CONCLUSIONS

Many advances have been made in tissue engineering research, and biological wound dressings are undoubtedly one of the most successful alternative materials yet produced. In our study, we verified that the CL/CS and

SF/CS nanofiber scaffolds have good biocompatibility both *in vitro* and *in vivo*. *In vitro*, the proliferation of cells on the CL/CS and SF/CS nanofiber scaffolds and tissue culture plastic was assessed at different times by MTT assays, and there were significant differences in cell

growth between the nanofiber scaffold and control groups after 3, 5, and 7 days of culture. The morphology of cells cultured on the CL/CS and SF/CS nanofiber scaffolds for seven days was clearly observed by SEM. *In vivo*, we verified that the CL/CS and SF/CS nanofiber scaffolds were more suitable as biological wound dressings than traditional gauze. In summary, these CL/CS and SF/CS nanofiber scaffolds greatly promote wound healing; therefore, while further research is necessary, these two types of scaffolds have great potential for use in skin tissue engineering applications.

Acknowledgments: This research was supported by the National High Technology Research and Development Program of China under Grant 2008AA03Z305, P. R. China. This research was also supported by the Shanghai Municipal Commission of Health and Family Planning under Grant 20154Y0198, P. R. China. The funding support did not create any conflicts of interest regarding the publication of this manuscript, and there were no other possible conflicts of interest related to this article.

References and Notes

- C. Cochran, M. G. Rippon, A. Rogers, R. Walmsley, D. Knottenbelt, and P. Bowler, Application of an *in vitro* model to evaluate bioadhesion of fibroblasts and epithelial cells to two different dressings. *Biomater* 20, 1237 (1999).
- L. Bao, W. Yang, X. Mao, S. Mou, and S. Tang, Agar/collagen membrane as skin dressing for wounds. *Biomed. Mater.* 3, 044108 (2008).
- S. B. Mahjour, X. Fu, X. Yang, J. Fong, F. Sefat, and H. Wang, Rapid creation of skin substitutes from human skin cells and biomimetic nanofibers for acute full-thickness wound repair. *Burns* 41, 1764 (2015).
- N. Hanifi, A. S. Halim, C. F. Aleas, J. Singh, M. Marzuki, T. T. Win, L. C. Keong, T. P. Kannan, and A. A. Dorai, Epidermal regeneration of cultured autograft, allograft, and xenograft keratinocytes transplanted on full-thickness wounds in rabbits. *Exp. Clin. Transplant.* 13, 273 (2015).
- T. T. Nyame, H. A. Chiang, T. Leavitt, M. Ozambela, and D. P. Orgill, Tissue-engineered skin substitutes. *Plast. Reconstr. Surg.* 136, 1379 (2015).
- G. Rath, T. Hussain, G. Chauhan, T. Garg, and A. K. Goyal, Collagen nanofiber containing silver nanoparticles for improved wound-healing applications. *J. Drug Target.* 24, 520 (2016).
- C. Helary, A. Abed, G. Mosser, L. Louedec, D. Letourneur, T. Coradin, M. M. Giraud-Guille, and A. Meddahi-Pellé, Evaluation of dense collagen matrices as medicated wound dressing for the treatment of cutaneous chronic wounds. *Biomater. Sci.* 3, 373 (2015).
- J. A. Matthews, G. E. Wnek, D. G. Simpson, and G. L. Bowlin, Electrospinning of collagen nanofibers. *Biomacromolecules* 3, 232 (2002).
- R. L. Horan, K. Antle, A. L. Collette, Y. Wang, J. Huang, J. E. Moreau, V. Volloch, D. L. Kaplan, and G. H. Altman, *In vitro* degradation of silk fibroin. *Biomater.* 26, 3385 (2005).
- A. H. Teuschl, L. Neutsch, X. Monforte, D. Rünzler, M. van Griensven, F. Gabor, and H. Redl, Enhanced cell adhesion on silk fibroin via lectin surface modification. *Acta Biomater.* 10, 2506 (2014).
- L. Meinel, S. Hofmann, V. Karageorgiou, C. Kirker-Headf, J. McCool, G. Gronowicz, L. Zichner, R. Langer, G. Vunjak-Novakovic, and D. L. Kaplan, The inflammatory responses to silk films *in vitro* and *in vivo*. *Biomater.* 26, 147 (2005).
- L. Mei, D. Hu, J. Ma, X. Wang, Y. Yang, and J. Liu, Preparation, characterization and evaluation of chitosan macroporous for potential application in skin tissue engineering. *Int. J. Biol. Macromol.* 51, 992 (2012).
- Y. H. Lin, J. H. Lin, T. S. Li, S. H. Wang, C. H. Yao, W. Y. Chung, and T. H. Ko, Dressing with epigallocatechin gallate nanoparticles for wound regeneration. *Wound Repair Regen.* 24, 287 (2016).
- S. Ladet, L. David, and A. Domard, Multi-membrane hydrogels. *Nature* 452, 76 (2008).
- A. Sionkowska, M. Wisniewski, J. Skopinska, C. J. Kennedy, and T. J. Wess, Molecular interactions in collagen and chitosan blends. *Biomater.* 25, 795 (2004).
- M. Montinaro, V. Fasano, M. Moffa, A. Camposeo, L. Persano, M. Lauricella, S. Succi, and D. Pisignano, Sub-ms dynamics of the instability onset of electrospinning. *Soft Matter* 11, 3424 (2015).
- B. S. Lee, S. Y. Jeon, H. Park, G. Lee, H. S. Yang, and W. R. Yu, New electrospinning nozzle to reduce jet instability and its application to manufacture of multi-layered nanofibers. *Sci. Rep.* 4, 6758 (2014).
- A. Edwards, D. Jarvis, T. Hopkins, S. Pixley, and N. Bhattarai, Poly(ϵ -caprolactone)/Keratin-based composite nanofibers for biomedical applications. *J. Biomed. Mater. Res. B Appl. Biomater.* 103, 21 (2015).
- A. Yin, K. Zhang, M. J. McClure, C. Huang, J. Wu, J. Fang, X. Mo, G. L. Bowlin, S. S. Al-Deyab, and M. El-Newehy, Electrospinning collagen/chitosan/poly(L-lactic acid-co- ϵ -caprolactone) to form a vascular graft: Mechanical and biological characterization. *J. Biomed. Mater. Res. A* 101, 1292 (2013).
- S. D. Sarkar, B. L. Farrugia, T. R. Dargaville, and S. Dhara, Chitosan-collagen scaffolds with nano/Microfibrous architecture for skin tissue engineering. *J. Biomed. Mater. Res. A* 101, 3482 (2013).
- A. Martínez, M. D. Blanco, N. Davidenko, and R. E. Cameron, Tailoring chitosan/Collagen scaffolds for tissue engineering: Effect of composition and different crosslinking agents on scaffold properties. *Carbohydr. Polym.* 132, 606 (2015).
- Z. G. Chen, P. W. Wang, B. Wei, X. M. Mo, and F. Z. Cui, Electrospun collagen-chitosan nanofiber: A biomimetic extracellular matrix for endothelial cell and smooth muscle cell. *Acta Biomaterialia* 6, 372 (2010).
- K. Zhang, Y. Qian, H. Wang, L. Fan, C. Huang, and X. Mo, Electrospun silk fibroin-hydroxybutyl chitosan nanofibrous scaffolds to biomimic extracellular matrix. *J. Biomater. Sci. Polym. Ed.* 22, 1069 (2011).

Received: 17 August 2016. Accepted: 1 September 2016.